JMEPEG (2008) 17:842–848
DOI: 10.1007/s11665-008-9218-4

1059-9495/$19.00

Failure During Sheared Edge Stretching

B.S. Levy and C.J. Van Tyne

(Submitted January 29, 2008)

Failure during sheared edge stretching of sheet steels is a serious concern, especially in advanced high-strength steel (AHSS) grades. The shearing process produces a shear face and a zone of deformation behind the shear face, which is the shear-affected zone (SAZ). A failure during sheared edge stretching depends on prior deformation in the sheet, the shearing process, and the subsequent strain path in the SAZ during stretching. Data from laboratory hole expansion tests and hole extrusion tests for multiple lots of fourteen grades of steel were analyzed. The forming limit curve (FLC), regression equations, measurement uncertainty calculations, and difference calculations were used in the analyses. From these analyses, an assessment of the primary factors that contribute to the fracture during sheared edge stretching was made. It was found that the forming limit strain with consideration of strain path in the SAZ is a major factor that contributes to the failure of a sheared edge during stretching. Although metallurgical factors are important, they appear to play a somewhat lesser role.

Keywords formability, forming limit curve, sheared edge, sheet steel

1. Introduction

Failure in sheared edge stretching is a common limitation in the use of advanced high-strength steels (AHSS) that are increasingly being specified for automotive parts. Thus, for intelligent die design, the factors that cause failure in sheared edge stretching need to be understood. The present study provides insight on several of these factors and also provides an engineering methodology for predicting failure strains in sheared edge stretching.

The shearing process is characterized by a shear face and a zone of deformation behind the shear face, which is the shear-affected zone (SAZ). Understanding failure in sheared edge stretching requires consideration of the surface condition of the shear face as well as the effect of the SAZ on subsequent deformation. The SAZ has sustained substantial strain during shearing so that conditions leading to a ductile fracture process are well advanced prior to any stretching of the sheared edge. Since failure is related to forming limit behavior, the strain path in the SAZ is important. Thus, failure in sheared edge stretching is determined by the effect of prior deformation, the severity of the shearing process, and the subsequent strain path in the SAZ.

The failure of sheared edges during stretching has been studied by a number of investigators over the years. Adamczyk et al. (Ref 1, 2) has examined high-strength low alloy steel sheets. They found that high tensile strength was a detriment to expansion performance, whereas steels with higher elongation and higher planar anisotropy performed better. Comstock et al. (Ref 3) extended the work of Admczyk et al. to ferritic, ferritic stainless and austenitic stainless steels. Davies (Ref 4) observed that inclusions and poor quality edges decreased the edge ductility in high-strength low alloy steels. Milosevic and Moussy (Ref 5) found that strain hardening and cavity formation affected the critical fracture strain for the sheared edges of sheet steels. Although working with aluminum, Seo (Ref 6) showed details of sheared edge and a cross-sectional profile of the edge. He characterizes the various features seen in a sheared edge—fractures, burnishing, rollover, burrs, and work hardening in the adjacent area. (Note that his adjacent area corresponds to the SAZ described in this article.) Pradhan et al. (Ref 7) compared the edge performance behavior of dual phase steels with other steels of a low strength. The edge performance of other high-strength steels has been studied by Konieczny (Ref 8).

In this study, failure is described by using a regression equation with the Keeler-Brazier forming limit as the primary independent variable. Specific metallurgical effects are determined by using the difference between actual results for different steel grades and predicted results from the regression equation. The severity of the sheared edge forming process is analyzed using results for identical samples (1) with and without the removal of the shear burr and (2) with and without the removal of the shear burr and the SAZ. The effect of strain path on stretching a sheared edge is analyzed using results from identical samples deformed using either a flat or a conical punch.

2. The Shear-Affected Zone

Shearing produces two distinct but related types of damage: (1) surface damage that is characterized by areas with rollover, burnishing, fracture, and burrs; and (2) a SAZ that extends from the sheared surface into the adjacent metal. The SAZ is a volume of metal that has been subjected to substantial plastic deformation. Both the sheared surface and the SAZ can affect

B.S. Levy, B.S. Levy Consultants Ltd., 1700 E. 56th St., Suite 3705, Chicago, IL 60637; and **C.J. Van Tyne**, Department of Metallurgical and Materials Engineering, Colorado School of Mines, Golden, CO 80401. Contact e-mail: cvantyne@mines.edu.

failure in stretching a sheared edge. For a production stamping process, failure in sheared edge stretching is a combination of deformation in the sheet prior to shearing, damage associated with shearing, and subsequent stretching of the sheared edge. Even if the prior deformation in the sheet is nominal, the plastic deformation associated with shearing results in considerable strain in the SAZ—the conditions for a ductile fracture are well advanced before the sheared edge is stretched.

In sheared edge stretching, the strain path at a sheared edge is equivalent to the strain path in a tensile test. The component of strain perpendicular to the sheared edge can be determined from the normal anisotropy ($\bar{R}$) of the sheet and constancy of volume. In contrast, in the SAZ, the overall forming process affects the strain path, because the deformation associated with the overall forming process is generally different from that of a tensile test. It is expected that there are radial and circumferential strain component gradients in the SAZ. Since the SAZ affects sheared edge failure, the effect of these strain component gradients should be included in a generally applicable failure criterion.

The evaluation of sheared edge stretchability for a sheet steel is often determined by expanding a hole. Such laboratory tests are run using either a flat bottom punch (called a hole expansion test) or a conical punch (called a hole extrusion test). In these tests, a punch is pushed against or through the sheared hole with the perimeter of the blank fully restrained until fracture is observed. The increase in hole diameter is a quantitative measure used to assess sheared edge stretchability.

The effect of the sheared edge and the SAZ on failure limits determined from a hole expansion test with a flat bottom punch is shown in Table 1 (Ref 2, 9). The specific criteria for the failure strains in Table 1 are not given, but one would expect that the criterion is consistent for each individual investigation. It would also be expected that the specific failure criterion would use strains that are greater than those used in the experimental determination of a forming limit curve (FLC) for the same steel. The data in Table 1 indicate that when both the sheared edge and the SAZ are removed, the strain at failure is substantially larger. In contrast, removing only the shear burr has a modest effect on the strain at failure.

Keeler (Ref 10) has shown that as the height of a shear burr increases, the strain at failure decreases. Keeler's results suggest that shearing process variables that increase burr height also increase metallurgical damage in the SAZ. The relationship between shearing variables and metallurgical damage probably depends on specific shearing conditions.

Table 1 Effect of the sheared edge and the shear-affected zone on failure strain

			Apparent hole expansion[a]		
			True strain		
Steel grade	References	Thickness, mm	As sheared	Burr removed	Shear-affected zone removed
HSLA50A	2	1.45	0.52	XXX	0.99
HSLA50B	2	1.57	0.36	XXX	0.94
HSLA70	2	1.32	0.29	XXX	0.79
HSLA80	2	1.52	0.22	XXX	0.64
HSLA35	2	1.12	0.55	0.60	XXX
HSLA45	2	0.71	0.32	0.35	XXX
HSLA50A	9	0.78	0.36	0.48	XXX
HSLA50B	9	0.78	0.33	0.44	XXX
HSLA50C	9	0.78	0.55	0.55	XXX
HSLA60	9	1.45	0.37	0.38	XXX
RA70	9	1.27	0.24	0.26	XXX
RA80	9	1.08	0.22	0.21	XXX

[a]The failure criteria for these tests are not specified, but are likely to be different than the failure criterion that would be used in experimentally determining a forming limit curve

3. Forming Limit Curves

If the failure criterion for a hole expansion test and an experimentally determined FLC are similar, there should be a fundamental relationship between strain at failure strain ($\varepsilon_{\text{failure}}$) for a hole expansion test and the strain calculated from an FLC for the tensile strain path ($\varepsilon_{\text{FLC-limit}}$). The Keeler-Brazier equation, as modified by an NADDRG project (Ref 11, 12), can be used to calculate FLC_0, which is the forming limit for plane-strain conditions in engineering strain. The forming limit strain applies to a hole expansion test or a hole extrusion test with the shear damage removed. The true forming limit strain for a sheared edge is a useful first step in analyzing experimental data to determine the failure limit during stretching of a sheared edge.

The terminal strain-hardening exponent (terminal n-value) should be used in calculating FLC_0 (Ref 13). For standard tensile testing, the best measure of terminal n-value is the percent uniform elongation expressed in true strain.

The initial step in determining the FLC limit strain, $\varepsilon_{\text{FLC-limit}}$, is to calculate FLC_0, from the Keeler-Brazier equation (Ref 11) and convert it into true strain.

$$\varepsilon_{\text{FLC}_0} = \ln\left(1 + \frac{(23.3 + 14.14T)(n_t/0.21)}{100}\right) \quad \text{(Eq 1)}$$

where T is the sheet thickness in millimeters and n_t is the terminal strain hardening exponent.

Since the strain path at a sheared edge is equivalent to the strain path of a tensile test, $\varepsilon_{\text{FLC}_0}$ is multiplied by $(1 + \bar{R})$, where $\bar{R}$ is the normal anisotropy of the sheet steel, to determine the intersection of the tensile test strain path and the FLC curve. This calculation is:

$$\varepsilon_{\text{FLC-limit}} = (1 + \bar{R})\varepsilon_{\text{FLC}_0} \quad \text{(Eq 2)}$$

4. Data Analysis

The data for the subsequent analysis are from a study by Sriram et al. (Ref 14). In their study, special techniques were developed to match the failure criteria in the hole expansion and the hole extrusion tests with those used in experimentally determining FLCs (Ref 14). While it is not possible to verify that the failure limits for the hole expansion or the hole extrusion tests match the very shallow neck used in experimentally determining a FLC, this assumption is used in the present analysis.

Table 2 shows the steels in the study by Sriram et al. (Ref 14), and the material properties used in the subsequent analysis. Table 2 includes terminal *n*-values calculated from uniform elongation and where available, the *n*-value taken from 6 to 12% strain. Table 2 indicates that for some steels, terminal *n*-value can be significantly different from the 6 to 12% *n*-value. These differences between terminal *n*-value and 6 to 12% *n*-value are the result of variations in instantaneous *n*-value with strain.

Table 2 Material properties for data analysis

Grade	Lot code	Thickness, mm	Uniform elongation, %	*n*-Value terminal calculated	*n*-Value 6-12% experiment	$\bar{R}$
DQSK	X1	0.77	21.5	0.195	0.241	1.93
	X2	1.19	21.0	0.195	0.224	1.98
DDQ+	Y1	0.70	23.8	0.213	0.264	2.25
	Y2	1.19	23.5	0.211	0.274	2.15
BH210	B1	0.70	19.3	0.176	0.183	1.64
	B2	0.93	19.0	0.174	0.171	1.75
BH280	C1	0.71	17.9	0.165	0.168	1.13
	C2	1.00	16.0	0.148	0.157	1.47
	C3	1.04	19.5	0.178	0.184	1.00
ULCBH340	D1	0.74	18.0	0.166	0.168	2.08
	D2	1.02	21.2	0.192	0.206	1.54
IF Rephos	E1	0.63	22.0	0.199	0.237	1.90
	E2	0.89	22.2	0.200	0.239	1.83
DP500	G1	0.66	18.9	0.173	0.201	0.83
	G2	0.81	17.4	0.160	0.182	0.92
BH300	1K	1.24	16.5	0.153	0.179	1.04
	2K	1.19	18.5	0.170	0.179	1.60
HSLA350	1L	1.16	19.1	0.175	0.210	1.06
	5L	1.21	16.1	0.149	0.167	1.16
	2L	1.62	14.6	0.136	0.125	1.08
HS440W	1M	1.24	16.7	0.154	0.179	0.90
	2M	1.58	16.7	0.154	0.171	0.94
DP600	1P	0.96	16.0	0.149	0.182	0.86
	2P	1.19	15.7	0.146	0.180	0.84
	3P	1.39	16.2	0.150	0.188	0.87
	4P	1.23	13.9	0.130	0.147	0.93
	5P	1.64	18.5	0.170	0.244	1.01
	6P	1.49	13.8	0.129	0.144	1.00
TRIP600	1T	1.40	19.9	0.181	0.237	0.93
	2T	1.60	19.3	0.176	0.234	0.89
DP800	1R	1.20	10.7	0.102	N.A.	0.85
	2R	1.59	10.5	0.100	N.A.	0.85
DP980	1S	1.15	5.8	0.056	N.A.	0.80
	2S	1.52	6.0	0.058	N.A.	0.80

Although there is some controversy in using the Keeler-Brazier equation for steels other than low carbon, it has been found that if the terminal *n*-value is used then good results have been obtained using the Keeler-Brazier equation for a wide range of steel grades (Ref 15). FLCs for only three of the high-strength steels (TIRP600, RA830, and DP980) analyzed in the present study were experimentally determined (Ref 14). For these three steels the experimental FLC_0 and the FLC_0 calculated using the Keeler-Brazier equation exhibited reasonable agreement.

Tests to increase hole diameter using either a flat bottom punch (hole expansion) or a conical punch (hole extrusion) were used in the study (Ref 14). Sample preparation was identical for both tests with a 10% shear clearance used in piercing the holes. Figure 1 shows representative pictures for specimens stretched by both types of punches. Note that the crack in the test piece that was expanded with the conical punch (Fig. 1b) represents a fracture substantially in excess of the failure limit strain.

The majority of the tests were run using a conical punch, but a statistically reliable regression (Ref 14) relating results from the conical punch test to results from the flat bottom punch test is:

$$(\%\text{Hole Extrusion}) = -5.8152 + 1.3068\,(\%\text{Hole Expansion}) \quad \text{(Eq 3)}$$

The statistics for Eq 3 are excellent; the square of the correlation coefficient (R^2) is 0.997 and there is a random distribution of the data points about the regression line (Ref 14). However, it should be noted that the constant and coefficient in Eq 3 could be different if the tests were run on samples where the holes were produced with a different percent shear clearance.

The following analysis of the data is based on results for a flat punch, because conical punches are not normally used to experimentally determine FLCs. The experimental data for the conical punch tests and the values equivalent to a flat bottom punch test are shown in Table 3, where Eq 3 is used to convert the data.

The initial step in the analysis is to relate the failure strain ($\varepsilon_{\text{failure}}$) for the hole expansion test to $\varepsilon_{\text{FLC-limit}}$ for the tensile strain path calculated using Eq 2. The experimental hole expansion data are related to the matching forming limit strain using the regression equation:

$$\varepsilon_{\text{failure}} = a_0 + a_1 \varepsilon_{\text{FLC-limit}} \quad \text{(Eq 4)}$$

with $a_0 = 0.019 \pm 0.075$ and $a_1 = 0.850 \pm 0.121$. The R^2 value for Eq 4 is 0.61. Figure 2 shows the relationship between $\varepsilon_{\text{failure}}$ and $\varepsilon_{\text{FLC-limit}}$.

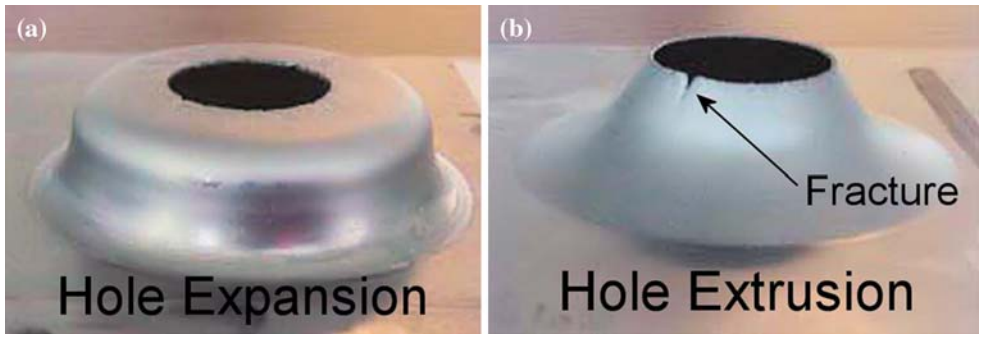

Fig. 1 Representative specimens from (a) a hole expansion test with a flat bottom punch and (b) a hole extrusion test with a conical punch (Ref 1). The crack in the hole extrusion test is from a sample that was tested beyond failure

Table 3 Experimental hole extrusion

Grade	Lot code	%Hole extrusion (conical punch) Average	Std Dev	Std Dev/Ave	Calculated %hole expansion (flat bottom punch)[a]
DQSK	X1	145.1	9.0	0.062	115.5
	X2	152.1	16.0	0.105	120.9
DDQ+	Y1	150.5	5.7	0.038	119.6
	Y2	177.9	2.7	0.015	140.6
BH210	B1	152.0	2.8	0.019	120.7
	B2	151.5	4.7	0.031	120.3
BH280	C1	98.9	2.2	0.022	80.1
	C2	98.6	3.5	0.035	79.9
	C3	101.1	9.7	0.096	81.8
ULCBH340	D1	157.6	8.0	0.051	125.1
	D2	122.4	3.1	0.026	98.1
IF Rephos	E1	141.7	4.0	0.028	112.9
	E2	159.2	8.3	0.052	126.3
DP500	G1	56.0	5.6	0.099	47.3
	G2	57.2	6.6	0.115	48.3
BH300	1K	66.6	13.5	0.203	55.4
	2K	123.8	7.9	0.064	99.2
HSLA 350	1L	86.6	9.5	0.109	70.7
	5L	95.1	4.3	0.045	77.2
	2L	89.8	6.4	0.071	73.1
HS440W	1M	84.2	13.7	0.162	68.9
	2M	66.9	7.5	0.112	55.6
DP600	1P	38.0	3.8	0.099	33.6
	2P	51.1	3.8	0.074	43.6
	3P	29.3	2.5	0.085	26.9
	4P	36.6	2.8	0.077	32.5
	5P	32.7	2.5	0.075	29.5
	6P	29.8	1.7	0.058	27.3
TRIP600	1T	51.0	6.5	0.128	43.4
	2T	40.0	3.0	0.075	35.0
DP800	1R	21.9	2.6	0.116	21.2
	2R	18.7	2.2	0.118	18.8
DP980	1S	53.7	15.1	0.281	45.5
	2S	61.1	7.4	0.121	51.2

[a]Values used to calculate $\varepsilon_{failure}$ by converting to true strain

Since $\varepsilon_{failure}$ should be zero when $\varepsilon_{FLC\text{-}limit}$ is zero, the constant in Eq 4 should be zero, and it is approximately zero. The R^2 value for Eq 4 indicates that $\varepsilon_{FLC\text{-}limit}$ accounts for 61% of the variation in the experimental failure strain data.

The measurement uncertainty for the data is calculated as:

$$U = \sqrt{U_{\varepsilon_{failure}}^2 + (0.85U_{\varepsilon_{FLC-limit}})^2} \quad \text{(Eq 5)}$$

where U is the measurement uncertainty for the regression equation. $U_{\varepsilon_{failure}}$ and $U_{\varepsilon_{FLC-limit}}$, respectively, are the measurement uncertainties associated with the failure strain and the forming limit strain, and the factor 0.85 is taken from Eq 4.

Sriram et al. (Ref 14) include data for the percent increase in hole diameter for the hole extrusion test (conical punch) that are needed to estimate the standard deviation applicable to $U_{\varepsilon_{failure}}$. The calculation is done by: (1) adding plus and minus the standard deviation to the average; (2) calculating true strains from these two engineering strain values; (3) determining the difference between the two true strain values; and (4) dividing the difference value by two. Table 4 shows the results of these calculations. Table 4 also shows that the standard deviations are

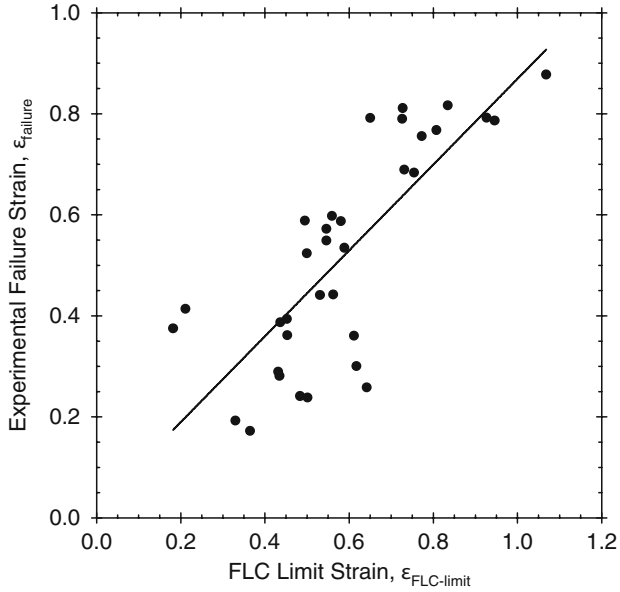

Fig. 2 Experimental failure strain at a sheared edge of hole expansion tests as a function of the calculated FLC limit strain

Table 4 Distribution of true strain standard deviations for each test lot (Ref 1)

Grade	Lot code	Hole Exp − Std Dev	Hole Exp + Std Dev	Difference/2
DQSK	X1	0.859	0.933	0.037
	X2	0.859	0.986	0.064
DDQ+	Y1	0.895	0.941	0.023
	Y2	1.012	1.032	0.010
BH210	B1	0.913	0.935	0.011
	B2	0.903	0.941	0.019
BH280	C1	0.677	0.698	0.011
	C2	0.668	0.704	0.018
	C3	0.649	0.746	0.048
ULCBH340	D1	0.915	0.977	0.031
	D2	0.785	0.813	0.014
IF Rephos	E1	0.866	0.899	0.017
	E2	0.920	0.984	0.032
DP500	G1	0.408	0.480	0.036
	G2	0.410	0.494	0.042
BH300	1K	0.426	0.589	0.081
	2K	0.770	0.840	0.035
HSLA 350	1L	0.572	0.673	0.051
	5L	0.646	0.690	0.022
	2L	0.606	0.674	0.034
HS440W	1M	0.534	0.682	0.074
	2M	0.466	0.556	0.045
DP600	1P	0.295	0.349	0.027
	2P	0.388	0.438	0.025
	3P	0.238	0.276	0.019
	4P	0.291	0.332	0.021
	5P	0.264	0.301	0.018
	6P	0.248	0.274	0.013
TRIP600	1T	0.367	0.454	0.043
	2T	0.315	0.358	0.022
DP800	1R	0.177	0.219	0.021
	2R	0.153	0.190	0.019
DP980	1S	0.326	0.523	0.099
	2S	0.430	0.522	0.046
Average =				0.033

Table 5 Summary of deviations from Eq 4

Steel grade	Lot code	Deviation Actual − Predicted	Std Dev for lot
Group 1			
DP600	5P	−0.307	0.018
TRIP600	2T	−0.244	0.022
DP600	3P	−0.207	0.019
DP600	6P	−0.189	0.013
TRIP600	1T	−0.179	0.043
DP800	2R	−0.158	0.019
DP600	4P	−0.108	0.021
DP800	1R	−0.107	0.021
DP600	1P	−0.097	0.027
DP600	2P	−0.043	0.025
	Ave	−0.164	0.023
	Std Dev	0.078	0.008
	Range −	−0.307	0.013
	Range +	−0.043	0.043
Group 2			
DDQ+	Y1	−0.037	0.023
DDQ+	Y2	−0.050	0.010
BH300	1K	−0.030	0.081
DQSK	X2	−0.014	0.064
DP500	G2	−0.010	0.042
DP500	G1	−0.003	0.036
ULCBH340	D2	0.023	0.014
BH300	2K	0.048	0.035
DQSK	X1	0.062	0.037
ULCBH340	D1[a]	0.174	0.031
	Ave	0.022	0.039
	Std Dev	0.067	0.022
	Range −	−0.037	0.010
	Range +	0.062	0.081
Group 3			
HS440W	2M	−0.055	0.045
HSLA350	1L	0.015	0.051
HSLA350	2L	0.065	0.022
BH280	C2	0.074	0.018
HS440W	1M	0.080	0.074
IF Rephos	E1	0.080	0.017
IF Rephos	E2	0.088	0.032
HSLA350	5L	0.089	0.022
BH280	C3	0.103	0.048
BH280	C1	0.148	0.011
	Ave	0.069	0.034
	Std Dev	0.054	0.020
	Range −	−0.055	0.011
	Range +	0.148	0.051
Group 4			
DP980	1S	0.201	0.099
DP980	2S	0.215	0.046
	Ave	0.208	0.072
	Std Dev	XXX	XXX

[a]This value not used in Ave and Std Dev

not normally distributed and that the average standard deviation is 0.033. Since $\varepsilon_{failure}$ for the hole extrusion tests are larger than $\varepsilon_{failure}$ for the hole expansion tests, the standard deviations for the conical punch tests are larger than for flat bottom punch tests. From Eq 3, for the estimation of $U_{\varepsilon_{failure}}$ for the hole expansion tests, the standard deviation for hole extrusion tests should be multiplied by 1/1.3068 or 0.765. Thus, $U_{\varepsilon_{failure}}$ is approximately 0.025.

For $U_{\varepsilon_{FLC-limit}}$, the combined effects of $\bar{R}$, terminal n-value, thickness, and inherent uncertainty in the FLC is estimated to be 0.03. The resulting measurement uncertainty, U, for Eq 5 is approximately 0.04 or 4%. In determining the measurement uncertainty inherent to Eq 4, the standard deviations for the experimental uncertainty should be doubled. Thus, the measurement uncertainty accounts for about 8% of the total data variation, and Eq 4 accounts for 61% of the total data variation. It is hypothesized that the remaining 31% of the variation can be attributed to differences in the metallurgical characteristics of the steels.

The effect of metallurgical characteristics is determined from a detailed analysis of the difference between the predicted values from Eq 4 and the actual experimental values. An analysis of these differences is shown in Table 5, where positive values indicate that the experimental value of $\varepsilon_{failure}$ is greater than that predicted by the regression analysis. Table 5 indicates that the steels can be grouped in four categories.

It can be seen from Table 5 that the Group 1 steels, DP600, DP800, and TRIP600, exhibit the greatest negative differences from that predicted by Eq 4, ranging from −0.307 to −0.043. The standard deviations for individual lots of steel are a significant fraction of the group standard deviation. It can also be seen that individual lots of the same steel grade are scattered through the ranking of Group 1. Thus, the metallurgical characteristics that affect sheared edge stretchability vary both among and within the steel grades. The magnitude of the difference term indicates that the microstructure for these steel grades is deleterious to sheared edge stretching.

The Group 2 steels are DDQ+, DQSK, BH300, ULCBH340, and DP500. They exhibit relatively little deviation from that predicted by the forming limit strain. The deviations range from −0.037 to 0.062 with an average value of 0.022. As with the Group 1 steels, the Group 2 steels do not separate by steel grade. Thus, while the Group 2 steels have different metallurgical characteristics, the effect on $\varepsilon_{failure}$ is similar.

The Group 3 steels are IF-Rephos, BH280, HSLA350, and HS440W. They exhibit some overlap with Group 2 steels, but the average difference is 0.069. As with Groups 1 and 2, there is no separation by steel grade.

Group 4 is DP 980, which exhibits an average deviation of 0.208. This value of the deviation indicates that the DP980 steels in this study exhibit considerably higher failure strains than would be predicted from Eq 4.

In summarizing results for the DP steels in the study (Ref 14), it can be seen that DP600 and DP800 exhibit failure strains that are much lower than predicted, DP500 exhibits failure strains that are similar to that predicted by the forming limit strain, and DP980 exhibits failure strains that are much greater than that predicted by Eq 4. The metallurgical causes for this behavior remain to be determined.

While specific metallurgical data are not available, it can be deduced from known microstructural characteristics of steel grades that the volume fraction hard phase, the strength differences between the hard and soft phases, and the coherence of the hard phase/soft phase interface probably contribute to the sheared edge failure.

5. Strain Path in the Shear-Affected Zone

The failure limit in true strain for a hole extrusion test with a 60° conical punch as a function of the FLC limit strain is described by the regression equation:

$$\varepsilon_{failure} = b_0 + b_1 \varepsilon_{FLC-limit} \quad \text{(Eq 6)}$$

with $b_0 = 0.003 \pm 0.09$ and $b_1 = 1.014 \pm 0.146$.

Since there is a direct relationship between hole expansion tests and hole extrusion tests with a 60° conical punch (Ref 14), the statistics for Eq 4 and 6 should be and are similar. For the same reason, the constant in Eq 6 should be and is essentially zero. If Eq 4 and 6 are compared, it can be seen that the coefficient in the regression equation for a 60° conical punch (i.e. Eq 6) is 1.01 compared to 0.85 for the regression equation for a flat punch (i.e. Eq 4). This difference in the coefficient values is the result of the strain path differences in the SAZ during the hole expansion test versus the hole extrusion test.

As discussed previously, the strain path in the SAZ is different from the strain path at the sheared edge. At the sheared edge, the strain path is equivalent to the strain path for a tensile test, where the radial strain component (ε_R) is equivalent to the width strain in a tensile test and the circumferential strain component (ε_C) is equivalent to the length strain in a tensile test. It should be noted that $\varepsilon_{FLC-limit}$ in Eq 4 and 6 is based on the strain path for the sheared edge.

The strain path on a forming limit plot is the ratio of the minor strain to the major strain. For the case of increasing the diameter of a sheared hole, the strain path is the ratio of ε_C to ε_R. The critical difference between a sheared edge and the SAZ is that there is stretching in the radial orientation in the SAZ that is not present at the sheared edge. Consequently, with more stretching, ε_R becomes less negative.

Since stretching with a flat punch (i.e. the hole expansion test) is "pure" stretching, it is postulated that there is more stretching for a hole expansion test than for a conical punch (i.e. hole extrusion test). With more stretching in the radial direction, ε_R is less negative for a hole expansion test than for a hole extrusion test. In contrast, ε_C is equal for the two tests, because it is a direct function of the increase in hole diameter. Thus, as Fig. 3 shows, the slope of the strain path on an FLC diagram for a hole extrusion test is to the left of the strain path for a hole expansion test. As a note, Fig. 3 does not consider the initial bending at the start of a hole extrusion test.

Since FLC is constant for any given material, the lower the slope of the strain path, the higher the intersection of the strain path and the FLC. This higher intersection point means that for a given material, $\varepsilon_{FLC-limit}$ is higher for a hole extrusion test than for a hole expansion test. This behavior explains the greater increase in hole diameter for hole extrusion tests than for hole expansion tests.

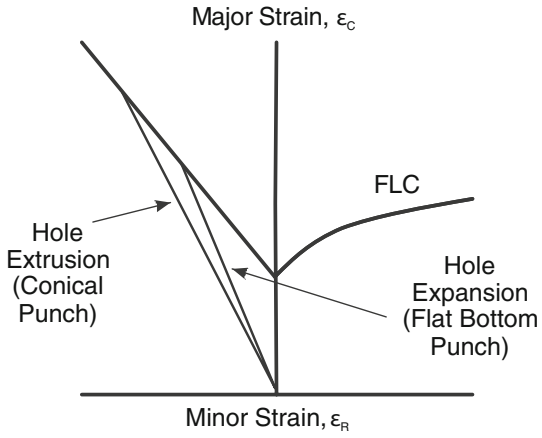

Fig. 3 Schematic representation of strain paths for hole extrusion test with a conical punch and a hole expansion test with a flat bottom punch on a forming limit plot

Figure 3 demonstrates that the strain path in the SAZ is needed to predict failure for sheared edge stretching in production parts. There is little or no evidence on the size of the SAZ or how it is affected by shearing conditions. Finite element analysis (FEA) with a fine mesh in the region adjacent to a sheared edge could provide a reasonable engineering approximation of the strain path for various forming conditions. It would also be desirable to experimentally determine the hardness and the size of the SAZ.

6. Summary

- The SAZ—the deformed region in the sheet adjacent to the sheared edge—must be considered when evaluating the failure strain in stretching a sheared edge.
- The forming limit strain calculated using the Keeler-Brazier equation with consideration of strain path in the SAZ is the dominant factor for determining failure strain of a sheared edge. Metallurgical considerations are also important, but appear to play a somewhat lesser role.
- The information contained in this study provides a framework for analyzing the results from tests that are used to evaluate sheared edge failures and applying these results to predicting failure in production stampings.

Acknowledgments

The authors thank the Auto/Steel Partnership in Southfield, MI, USA for partial support of this work. The authors also thank personnel at Ispat-Inland (now Arcelor Mittal) Research Laboratory in East Chicago, IL, USA for their work on the American Iron and Steel Institute project (Ref 14).

References

1. R.D. Adamczyk, D.W. Dickinson, and R.P. Krupitzer, The Edge Formability of High-Strength Cold Rolled Steel, *High Strength Steel for Automotive Use, Society of Automotive Engineers*, Warrendale, PA, USA, 1983, p 55–67
2. R.D. Adamczyk and G.M. Michal, Sheared Edge Extension of High Strength Cold Rolled Sheets, *J. Appl. Metalwork.*, 1986, **4**, p 157–163
3. R.J. Comstock, D.K. Scherre, and R.D. Adamczyk, Hole Expansion in a Variety of Sheet Steels, *J. Mater. Eng. Perform.*, 2006, **15**, p 675–683
4. R.G. Davies, Edge Cracking in High Strength Steels, *J. Appl. Metalwork.*, 1983, **2**, p 293–299
5. Z. Milosevic and R. Moussy, Simulation of Sheared Edge Behaviour in Stretch Flanging by a Modified Fukui Test, *Advanced Technology of Plasticity*, Vol. II, 1987, p 697–702
6. Y. Seo, Improving Blank Conditions in Progressive Stamping: Reducing Edge Defects Improves Subsequent Forming, *Stamping J.*, 2003, **15**, p 38–40
7. R.R. Pradhan, S.C. Kelley, and R.E. Fraley, Some Performance Aspects of Dual-Phase Steels in Comparison to HSLA, C-Mn and TRIP Steels, SAE Paper Number 2004-01-0505, SAE 2004 World Congress, 2004
8. A.A. Konieczny, On Formabiltiy Limitations in Stamping Involving Sheared Edge Stretching, SAE Paper Number 2007-01-0340, SAE 2007 World Congress, 2007

9. N. Lazaridus, Private Communication, November, 1986
10. S.P. Keeler, *Understanding Sheet Metal Formability, Part 5-Die Design and Lubrication, Machinery*, Vol. 74, no. 10, June, 1968
11. S.P. Keeler and W.G. Brazier, Relationship Between Laboratory Material Characterization and Press Shop Formability, *Proceedings of the Conference on Microalloying '75*, 1977, p 517–528
12. R. Soldaat, Private Communication, Unpublished Work of the NADDRG on the Keeler-Brazier Equation, circa early 1990s, December, 2000
13. S.P. Keeler, Private Communications on Proper *n* Value for Use in the Keeler-Brazier Equation, 1990-2000
14. S. Sriram, C. Wong, M. Huang, B. Yan, and D. Urban, Formability Characterization of a New Generation of High Strength Steels, Report No. 0012, American Iron and Steel Institute Technology Roadmap Program Office, Pittsburgh, PA, USA, 2003
15. B.S. Levy and D.E. Green, The Enhanced FLC Effect, Auto Steel Partnership Report, http://www.a-sp.org/database/pdf/Research%20Report.pdf, 2002